J Solid State Electrochem (2007) 11:593–599
DOI 10.1007/s10008-006-0204-1

ORIGINAL PAPER

An electrochemical study of safranin O binding to DNA at the surface

H. Heli · A. A. Moosavi-Movahedi · A. Jabbari · F. Ahmad

Received: 10 May 2006 / Revised: 29 May 2006 / Accepted: 11 July 2006 / Published online: 11 October 2006

Abstract The interaction of safranin O (SO) with double-stranded calf thymus DNA was investigated electrochemically, using a DNA-modified glassy carbon (GC-DNA) electrode. The results were compared with those obtained using a bare GC electrode. The formal potential of SO was more negative when using the GC-DNA electrode, although the rate of heterogeneous electron transfer was not altered. The GC-DNA electrode enabled preconcentration of the SO on the electrode surface, despite the fact that the mass transfer effects in the thin DNA layer adsorbed on the surface were still observed. The diffusion coefficient of SO and the binding ratio for the oxidized and reduced forms of the bound species were obtained. A binding isotherm for SO at the GC-DNA electrode was plotted from coulometric titrations, giving a binding constant of 5.8×10^4 L mol^{-1}.

Keywords DNA · Safranin O · Binding isotherm · DNA-modified electrode · Interaction

H. Heli · A. A. Moosavi-Movahedi (✉)
Institute of Biochemistry and Biophysics,
University of Tehran,
Tehran, Iran
e-mail: moosavi@ibb.ut.ac.ir

A. Jabbari
Department of Chemistry, Faculty of Science,
K. N. Toosi University of Technology,
Tehran, Iran

F. Ahmad
Department of Biosciences Jamia Millia Islamia,
New Delhi, India

Introduction

DNA is an immensely important material that plays an important role in life processes because it bears heritage information and instructs the biological synthesis of proteins and enzymes through the replication and transcription of genetic information in living cells. Studies of structure, binding specificity, mechanism, and dynamics of the interaction of small molecules with double helical DNA have attracted continuous interest in chemistry, physics, and biology. DNA binding molecules regulate mechanisms central to cellular function, including DNA replication and gene expression, especially those functions related to gene mutation, the origin of genetic diseases, and antitumor and antiviral drug mechanisms, thereby influencing our understanding of how proteins recognize and bind to specific DNA sequences [1, 2].

The binding of small molecules to DNA occurs through three major modes [3, 4]: electrostatic interactions with the negative-charged nucleic sugar–phosphate structure, binding interactions with the two grooves of the DNA double helix, and intercalation between the stacked base pairs of native DNA. The interactions between small molecules and DNA have been widely studied using various spectroscopic [5–10], calorimetric [11, 12], and electrochemical methods [13–15]. Electrochemical studies of these interactions have recently received a good deal of attention due to their low cost and the use of simpler and smaller devices with respect to the spectroscopic methods. On the other hand, the interpretation of electrochemical data can help elucidate the mechanisms by which drugs interact with DNA, similar to that which occurs in vivo [16]. These have focused primarily on the solution-phase phenomena, in which DNA-induced changes in the redox potential and/or

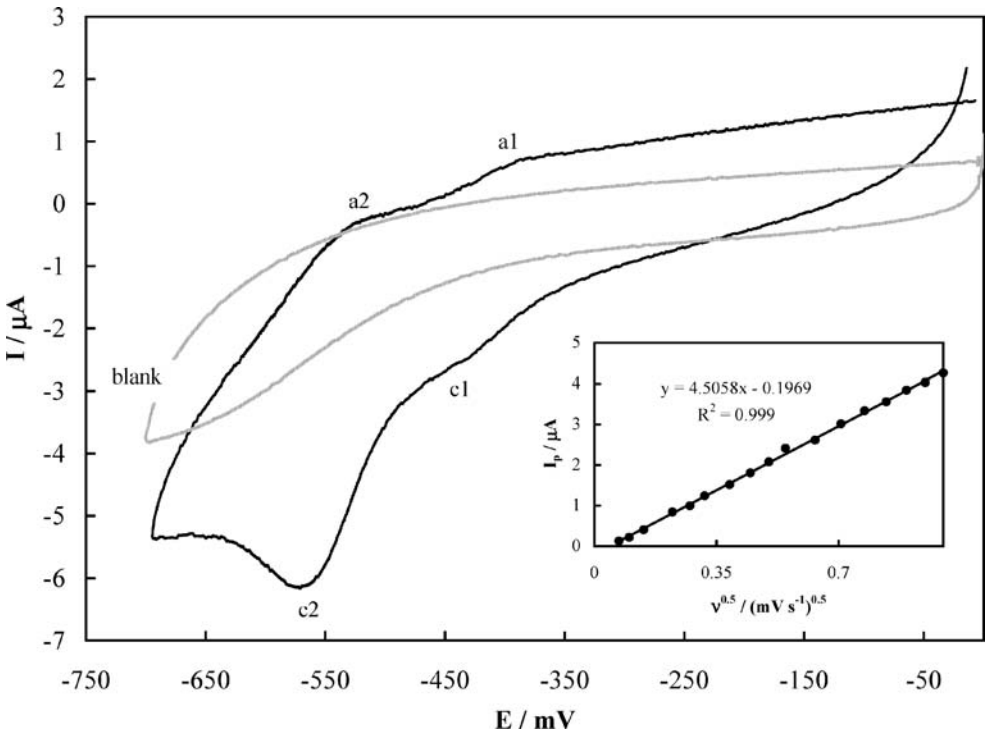

Fig. 1 *Main panel*: cyclic voltammogram obtained using a bare GC electrode: 200 μM SO in 0.05 M Tris–HCl solution, pH 7.4, potential range: 0 to −700 mV, potential sweep rate was 50 mV s^{-1}. *Inset*: changes in the reduction peak currents vs the corresponding square root of the potential sweep rate

diffusion characteristics of molecules have been analyzed [17, 18].

The applications of film electrodes are being investigated intensively. Electrodes coated with a film of DNA, usually in a solution/film/substrate arrangement, have been used in the study of ligand–DNA interactions [14, 19–21]. Redox reactions in the π-stack are particularly important for understanding charge delocalizations in DNA and their effect on base damage [22–24]. Meanwhile, recent photochemical studies suggest that the extended DNA π-stack facilitates long-range oxidative base damage [25].

Safranin O (SO) is a phenazine dye, which is similar to other planar dyes with chemical structures classified in the acridine, thiazine, and xanthene groups. Phenazine derivatives are known to inhibit bacterial growth, and some phenazium dyes have antimalarial potency [26]. Organic dyes can also serve to probe the structures and functions of biological macromolecules and are used to study some biophysical processes [27], as well as to mediate the electron transfer process in bioelectrocatalytic processes [28]. Studies on the interaction between phenazines and DNA may clarify the mechanism of biological activities of these compounds at the biomolecular level. The interaction of safranin T with DNA has been studied spectroscopically [29, 30]; however, electrochemical studies of the mechanism of the interaction between SO and DNA have not appeared in the literature.

Following our recent studies on the interactions of DNA with small molecules [11–14], electrochemical methods have been applied to the study of the interaction between SO and DNA.

Experimental

Double-stranded calf-thymus DNA (Sigma, St. Louis, MO, USA) was dissolved in 0.05 M Tris–HCl buffer at pH 7.4. Analytical grade HCl, SO, NaCl, and tris(hydroxymethyl) aminomethane (Merck, Whitehouse Station, NJ, USA) were used without further purification. All solutions were prepared with double-distilled water.

Electrochemical studies were carried out using the Autolab PGSTAT30 potentiostat/galvanostat (Eco Chemie, Utrecht, The Netherlands) equipped with a 5-mL cell incorporated three-electrode configuration containing 0.05 M Tris–HCl buffer (as the running electrolyte) at pH 7.4, unless otherwise stated. The system was run by a PC using GPES 4.9 software. In all voltammetric measurements, the IR drop compensation was performed by positive feedback. An Ag/AgCl (saturated KCl) electrode and a glassy carbon (GC) electrode were used as reference and counter electrodes, respectively. A GC disk electrode (Metrohm, Herisau, Switzerland), 2 mm in diameter (modified or otherwise), was used as a working electrode. All studies were carried out at room temperature.

The GC electrode was polished with 0.05 μm α-alumina powder on a piece of damp cotton wool. The electrode was then rinsed thoroughly with doubly distilled water prior to

modification. Films of DNA were created on the GC surface by transferring 5–7 μL of 0.5–1.0 mg mL^{-1} DNA solution to the surface of the electrode, which was allowed to dry under a warm flow of air (approximately 50 °C). The modified electrode was transferred to the running electrolyte, and a potential of 1,300 mV was applied for 5 min, followed by a sweeping of potential of 0 to 1,300 mV in a regime of cyclic voltammetry, as pretreatment to obtain reproducible results. The electrode, thus prepared, is hereafter referred to as a GC-DNA electrode throughout this report.

Potentiostatic chronocoulometric measurements were carried out using the GC-DNA electrode in SO-containing and SO-free solutions to obtain the values of capacitive (double-layer) charges, faradaic charges (related to the reduction of the adsorbed SO at the surface of the GC-DNA electrode), and the Cottrellian component of the transient currents. The potential was stepped from open circuit to −615 mV, which is sufficiently negative to enforce a mass transport-controlled current, for 100 s.

Results and discussion

Figure 1 represents a cyclic voltammogram of 200 μM SO in the buffer solution using a bare GC electrode in the potential range of 0 to −700 mV, with a potential sweep rate of 50 mV s^{-1}. SO underwent two redox transitions and was reduced in the cathodic half cycle with current peak positions at about −453 and −587 mV (denoted as c1 and c2, respectively) and its oxidation reaction is represented by two peaks at approximately −379 and −532 mV (denoted as a1 and a2) in the anodic potential sweep. The voltammogram is in good agreement with those previously reported [31, 32]. The probable redox transitions can be represented as follows:

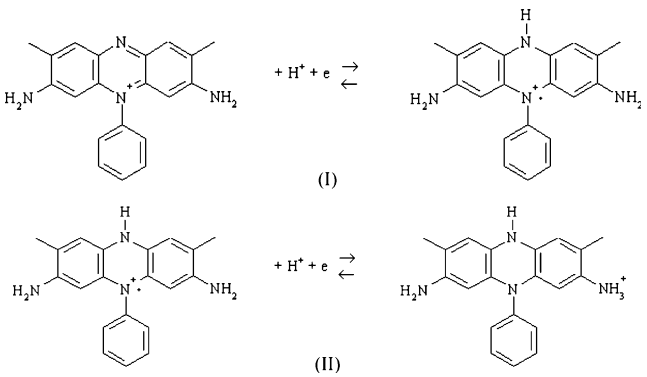

In the voltammogram shown in Fig. 1, the formal potential of second transition, $E^{0\prime}_{bulk}$, is about −540 mV and the peak potential separation is 60 mV with a potential sweep rate of 50 mV s^{-1} for the one-electron exchange reaction, indicating fast charge transfer kinetics. As shown in the inset of Fig. 1, for the cyclic voltammograms for SO in buffer solution recorded at different potential sweep rates at a bare GC electrode, the peak current c2 vs the corresponding square root of the potential sweep rate gave a linear plot. This indicates the occurrence of a mass transport phenomenon via diffusion in the rate-limiting step of the overall process. By using the slope of the plot, based on the Randles–Sevcik equation [33], the diffusion coefficient of SO in aqueous solution is 7.11×10^{-6} cm^2 s^{-1}.

Figure 2 shows the selected consecutive cyclic voltammograms of 200 μM SO in buffer solution using a GC-DNA electrode with a potential sweep rate of 50 mV s^{-1}. The currents of both peaks appeared in the voltammograms, confirming the oxidation and reduction of SO on the DNA-modified surface.

Figure 3 shows the cyclic voltammogram of 200 μM SO in the buffer solution after 100 cycles using a GC-DNA electrode and bare GC electrode. SO is represented by well-defined peaks in the voltammogram with higher currents using the GC-DNA electrode. The current of the redox couple of SO increased by about twofold, which indicates that by immobilizing DNA on the GC electrode, the DNA interaction with SO is enriched. The long-term response in the SO solution showed higher peak currents using the modified electrode, which reached maximum values after 100 cycles, with reduction and oxidation peak currents about 1.5 and 1.2 times higher for peaks c2 and a2, respectively, compared to those obtained using the bare electrode.

In the cyclic voltammograms of SO using the GC-DNA and GC electrodes (Fig. 3), the formal potential of SO at the GC-DNA electrode, $E^{0\prime}_{surf}$, was −560 mV. Thus, $E^{0\prime}_{surf}$ shifted by 20 (±2.2) mV to more negative potentials with respect to $E^{0\prime}_{bulk}$. This shift indicates that the oxidized form of SO interacts with DNA more strongly than the reduced form. However, the peak separation of the redox transition of SO is not altered using GC-DNA electrode, indicating that the heterogeneous charge transfer kinetics is not altered on the modified surface. The negative difference between the values of $E^{0\prime}_{surf}$ and $E^{0\prime}_{bulk}$ also revealed that the electrostatic attractions between SO and DNA, in the long run, overcame the intercalative attractions and stacking interactions [34, 35]. In the range of 4.2 to 142 mM, when the ionic strength of the solution was altered (by diluting of Tris–HCl buffer or the addition of NaCl), the difference between the formal potential of SO obtained using the bare GC electrode and that using the GC-DNA electrode in the same solutions ($\Delta E^{0\prime}$) decreases with increasing ionic strength (Table 1). This indicates that the intercalative

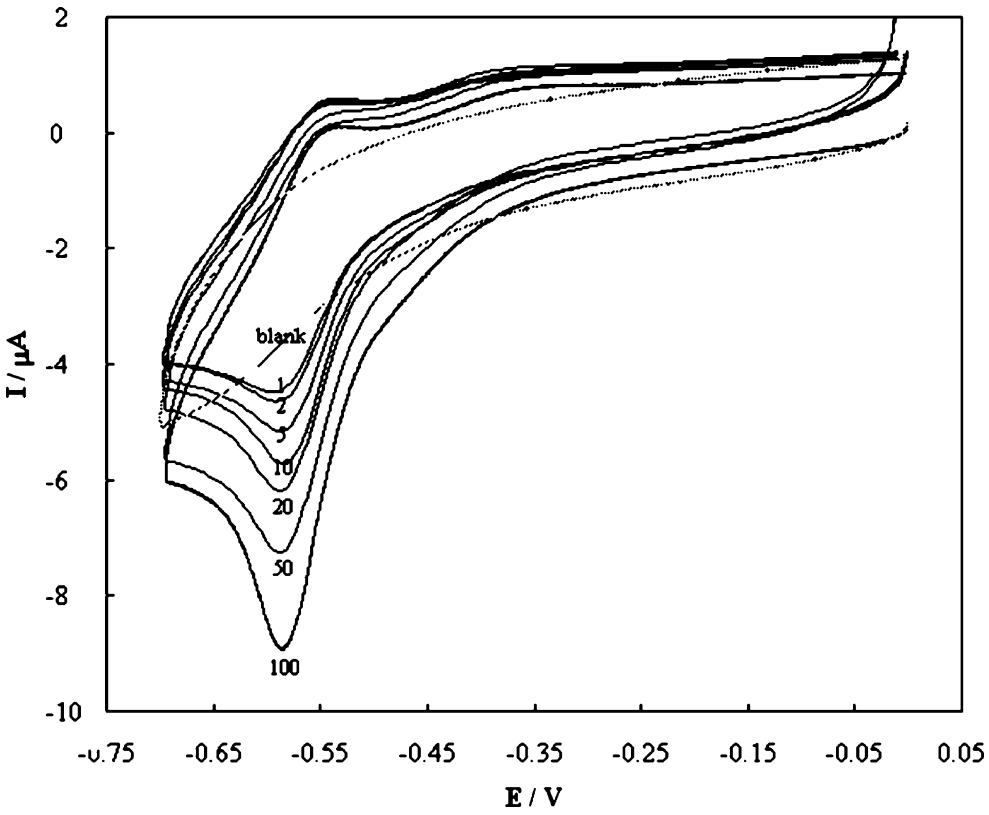

Fig. 2 Sampled consecutive cyclic voltammograms using a GC-DNA electrode: 200 μM SO in 0.05 M Tris–HCl solution, pH 7.4, potential sweep rate: 50 mV s^{-1}. The cycle number is indicated on each voltammogram

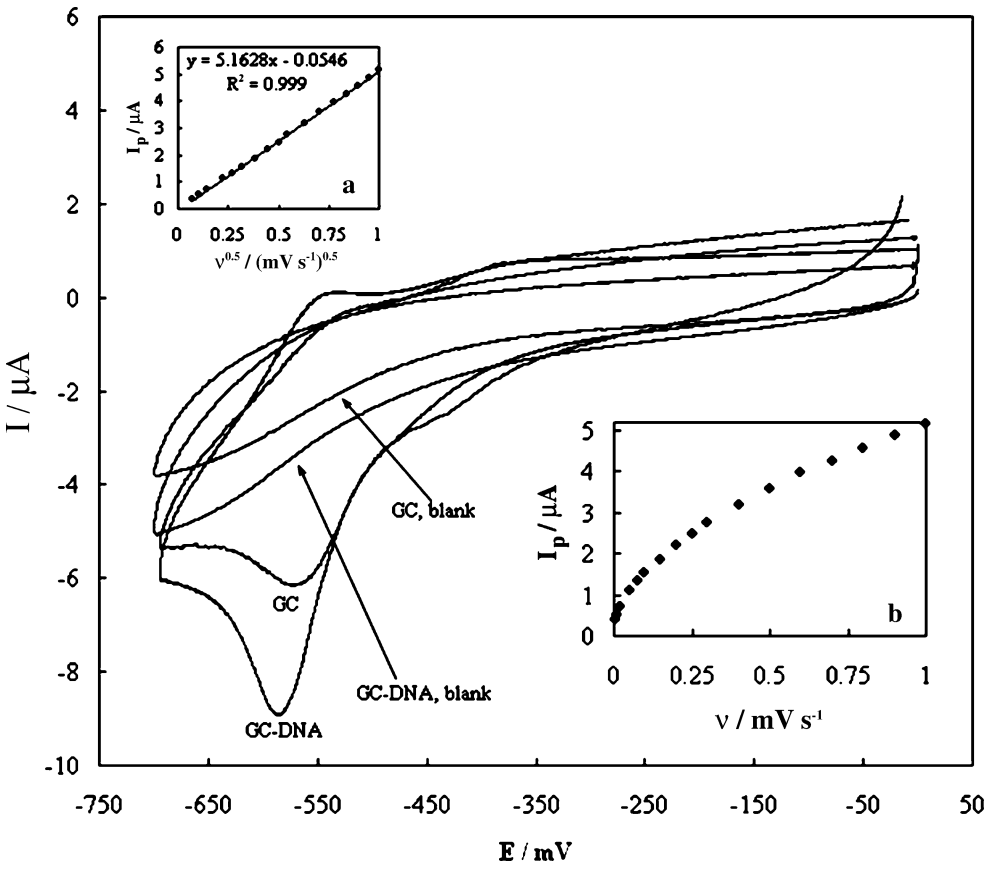

Fig. 3 *Main panel*: cyclic voltammograms of 200 μM SO after 100 cycles in buffer solution at GC-DNA and bare GC electrodes. The blank voltammogram was recorded using two electrodes. **a** Variations of the reduction peak currents of SO with the square root of potential sweep rate using the GC-DNA electrode in 200 μM SO buffer solution. **b** Variations of the reduction peak currents of SO with the potential sweep rate using the GC-DNA electrode in 200 μM SO buffer solution

Table 1 Dependency of the formal potential difference of the second transition of SO (the difference between the formal potential of SO obtained using GC and GC-DNA electrodes in the same solutions) with ionic strength of the solution

Ionic strength (M)	$\Delta E^{0\prime}$ (mV)
0.0042	−36 (±2.1)
0.0126	−31 (±1.7)
0.0252	−29 (±2.6)
0.042	−20 (±2.2)
0.047	−17 (±2.4)
0.052	−16 (±1.9)
0.062	−15 (±2.0)
0.092	−14 (±2.4)
0.142	−13 (±2.2)

attractions between SO and DNA in the solution with higher ionic strength are comparable to the electrostatic interactions [35].

For SO on the GC-DNA electrode in the range of 5 to 1,000 mV s^{-1}, peak current c1 has a linear relationship with the square root of the potential sweep rate (Fig. 3a), but not with the potential sweep rate (Fig. 3b). This linear dependency of peak currents on the square root of the potential sweep rate indicates that the redox transition of SO at the GC-DNA electrode is under mass transport control. Although it seems that SO is easily adsorbed onto the GC-DNA electrode surface (Fig. 2), the results indicate that a mass transport process occurred in the rate-limiting step of the redox process of SO at the GC-DNA electrode (see Fig. 3a). Moreover, this linear dependency is very similar to that obtained using a bare GC electrode (Fig. 1, inset). The same value was obtained for the product of $C{\times}D^{1/2}$, where C and D are the concentration and the diffusion coefficient, respectively, in the Randles–Sevcik equation, using the two electrodes. From the cyclic voltammograms depicted in Fig. 2, the concentration of SO must be higher on the GC-DNA electrode surface compared to that of the bulk of solution. Therefore, the diffusion coefficient of SO must be lower when using the GC-DNA electrode, because the $C{\times}D^{1/2}$ product remains the same. Because the mass transfer process is not target-surface-dependent, it can be concluded that mass transport occurs by diffusion in the thin layer of swollen DNA on the electrode surface. Thus, the concentration of SO is higher on the DNA-layer/solution interface, due to the interaction of DNA with SO, and SO diffuses through the DNA layer. The electron transfer process occurs in the DNA helix via electron/hole jumping through guanine bases that are parallel to the helix axis [36, 37]. However, the adsorption of the DNA on the GC surface via the interaction of exposed bases and/or external phosphate groups is random and thus cannot form the required regular network of parallel conducting wires.

After continuous potential sweeps (cyclic voltammogram with the highest peak currents depicted in Fig. 2), the currents of oxidation and reduction of SO on the GC-DNA electrode reached constant values. The electrode was rinsed rapidly with water and buffer solution and placed immediately in the SO-free solution, and consecutive cyclic voltammograms were then recorded (data not shown). The redox peaks became gradually lower, until constant but low values were achieved. This indicates the gradual dissociation of SO from DNA on the electrode surface into the SO-free solution. Time dependence of the cathodic peak current c2 (for SO bound to the double helical DNA) on the electrode surface obtained in the SO-free solution is given in Fig. 4. The logarithm of the reduction peak current depends linearly on the dissociation time, illustrating that the dissociation of SO obeys first-order reaction kinetics. The dissociation rate constant for SO was $5.67{\times}10^{-5}$ s^{-1}, with a half-time of 3.4 h. The dissociation of SO bound to the electrode surface can be expressed by first-order reaction kinetics as follows:

$$GC - DNA - SO \xrightarrow{k_d} GC - DNA + SO \quad (1)$$

Considering the Nernst equations for reversible redox reactions of free and bound species of SO (Scheme 1), the equality of thermodynamic potentials and the corresponding equilibrium constants for the binding of each oxidation state to the DNA layer can be expressed as follows [35, 38]:

$$\Delta \mathrm{E}^{0\prime} = \mathrm{E}^{0\prime}_{\mathrm{surf}} - \mathrm{E}^{0\prime}_{\mathrm{bulk}} = RT/\mathrm{nF}\, ln(K_{red}/K_{ox}) \quad (2)$$

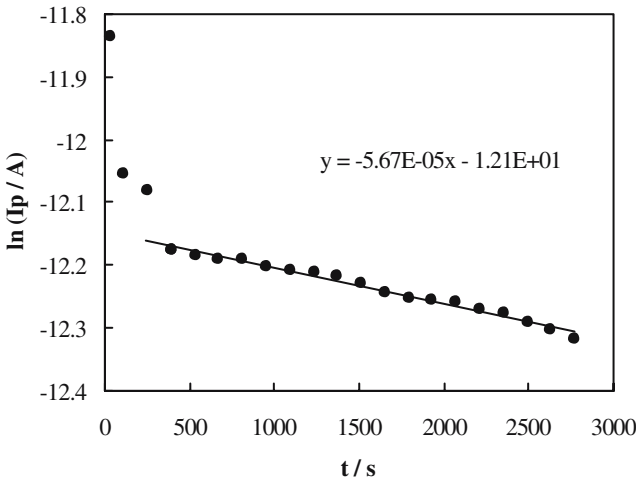

Fig. 4 Time variation of the logarithm of the second cathodic peak currents of SO bound to the GC-DNA electrode surface in SO-free buffer solution. When the current of the second reduction peak of SO reached its maximum value after 100 continuous cyclic voltammograms, the SO-bound GC-DNA electrode was rinsed rapidly with water and buffer solution and placed immediately in the buffer solution with no SO. Then, consecutive cyclic voltammograms were recorded. Each point is the logarithm of the time-dependent reduction peak current of SO bound to GC-DNA electrode in SO-free solution

where R is the universal constant of gases, F is the Faraday constant, and T is the absolute temperature. For a limiting shift of −20 (±2.2) mV, a ratio of K_{ox}/K_{red}=2.2 for SO was obtained. This ratio indicates that the interaction of the oxidized form of SO with the GC-DNA was more than two times stronger than that of the reduced form.

The affinity of SO for the DNA-modified surface was determined using chronocoulometry. The binding isotherm for SO, the relationship between the coulometric charge for SO bound to the GC-DNA electrode and its bulk concentration, is presented in Fig. 5. These data are described by Langmuir's model using the following equation [39]:

$$C_{bulk}/\Gamma_{ads} = C_{bulk}/\Gamma_{max} + 1/(K\Gamma_{max}) \quad (3)$$

where C_{bulk} and Γ_{ads} are the concentrations of SO in the bulk of the solution and adsorbed at the surface and K and Γ_{max} are the surface-binding constant and surface maximum binding for SO, respectively. The good fit obtained with this model is represented in the inset of Fig. 5, which confirms the independent noncooperative binding sites for SO on the DNA double helix, and gives K=5.8×10^4 L mol^{-1} and Γ_{max}=9.7×10^{-12} mol cm^{-2}.

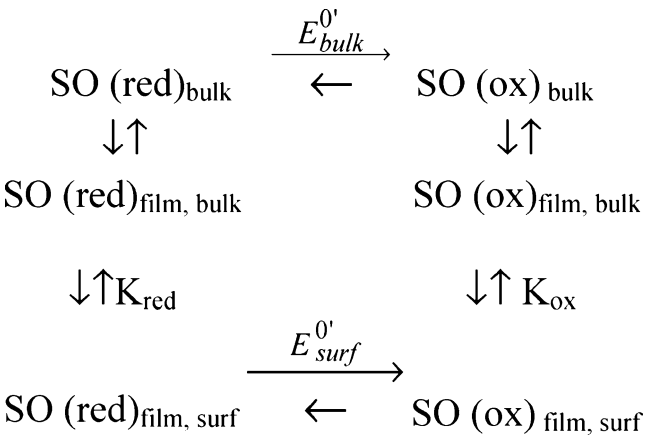

Scheme 1 Illustration of the process of the dissociation of SO, where *SO (ox)* and *SO (red)* represent the oxidized and reduced forms of the redox species, respectively. The subscripts *bulk*, *film, bulk*, and *film, surf* represent the species in the bulk of the solution, the species in the bulk of the DNA film, and the species bound to the electrode surface, respectively; K_{ox} and K_{red} are the corresponding binding constants for the oxidized and reduced forms of the redox species, respectively

Conclusion

We characterized the electrochemical behavior of SO in Tris–HCl buffer, pH 7.4, and the interaction between double helical DNA as a film adsorbed onto a GC surface and SO molecules using electrochemical methods. The

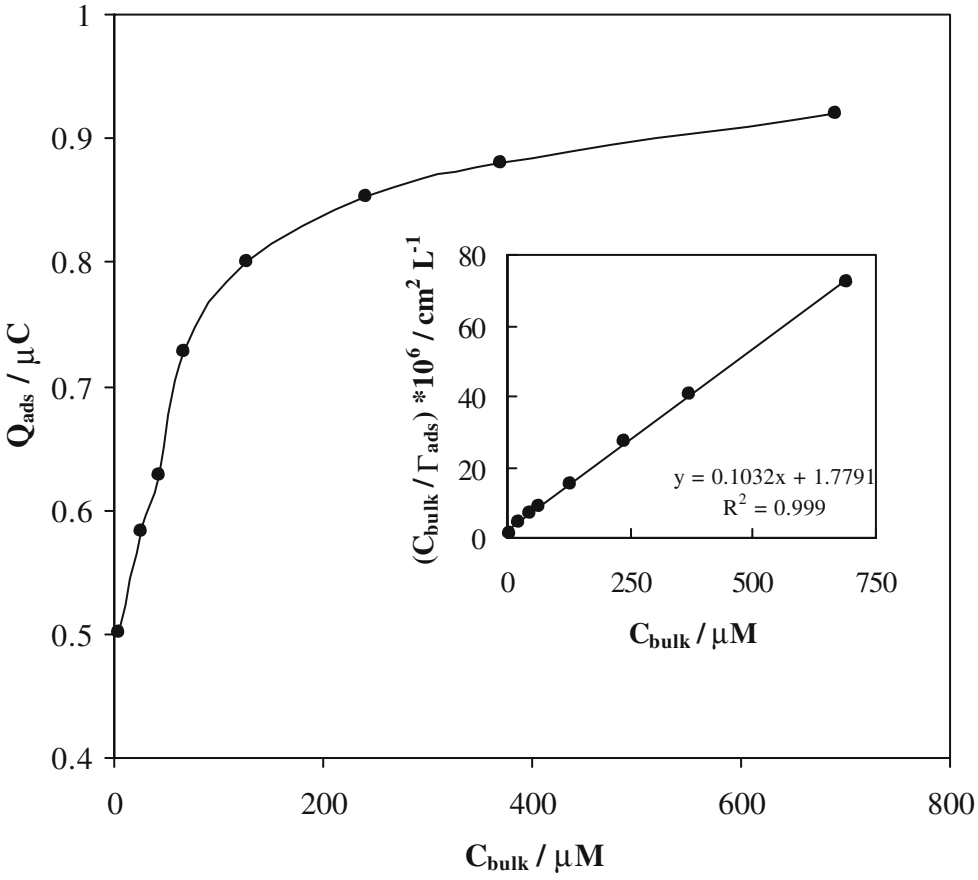

Fig. 5 *Main panel*: a binding isotherm for SO: plot of surface adsorption charge for SO to GC-DNA electrode vs concentration of SO in solution. Each point was obtained from potentiostatic chronocoulometric measurements after corrections for charging currents by measurements in SO-free solutions and Cottrellian currents. The potential was stepped from open circuit to −615 mV for 100 s. *Inset*: plot of C_{bulk}/Γ_{ads} vs C_{bulk} for the SO–DNA binding isotherm (*main panel*). The adsorbed concentrations of SO were calculated from Faraday's law

redox transition of SO is controlled by diffusion in the bulk of the solution. Furthermore, the DNA-modified GC electrode is a valuable tool in the examination of the redox behavior of a species within the DNA environment. The electrochemistry of DNA-modified surfaces provides a convenient method to determine equilibrium binding parameters of redox-active species. When using the DNA-modified electrode, the formal potential of redox-active species (as the mid peak potential) shifts to more negative potentials. Binding of SO to DNA can be described with a Langmuir isotherm deduced from coulometric charges for SO–DNA binding. The binding constant of SO to DNA, the dissociation of the species bound to DNA, and the ratio of binding constant for the oxidized vs reduced forms of SO were obtained using this method.

Acknowledgements The financial support of the Research Council of the University of Tehran and the Iran National Science Foundation are gratefully acknowledged.

References

1. Lane AN, Jenkins TC (2000) Q Rev Biophys 33:255–306
2. Sutherland IO (1986) Chem Soc Rev 15:63–91
3. Waring MJ (1981) Ann Rev Biochem 50:159–192
4. Gale EF, Cundliffe E, Reynold PE, Richmond MH, Waring MJ (1981) The molecular basis of antibiotic action. Wiley, London
5. Coates CG, Jacquet L, McGarvey JJ, Bell SE (1997) J Am Chem Soc 119:7130–7136
6. Becker HC, Norden B (1999) J Am Chem Soc 121:11947–11952
7. Marincola FC, Casu M, Saba G, Lai A (2001) ChemPhysChem 2:569–575
8. Kinoshita N, Yamamura T, Teranuma H, Katayama T, Tamanyu M, Negoro T, Satoh K, Sakagami H (2002) Anticancer Res 22:4017–4022
9. Aminzadeh A (2003) Iran J Chem Chem Eng 22:9–11
10. Marty R, Ouameur AA, Neault JF, Nafisi S, Tajmir-Riahi HA (2004) DNA Cell Biol 23:135–140
11. Nazari K, Golchin AR, Moosavi-Movahedi AA, Saboury AA, Hakimelahi GH, Shockravi A, Tangestani-nejad S (2005) Thermochim Acta 428:157–163
12. Moosavi-Movahedi AA, Golchin AR, Nazari K, Chamani J, Saboury AA, Bathaie SZ, Tangestani-Nejad S (2004) Thermochim Acta 414:233–241
13. Heli H, Bathaie SZ, Mousavi MF (2005) Electrochim Acta 51:1108–1116
14. Heli H, Bathaie SZ, Mousavi MF (2004) Electrochem Commun 6:1114–1118
15. Palecek E, Fojta M, Jelen F, Vetterl V (2002) In: Wilson GS (ed) Encyclopedia of electrochemistry, vol 9. Wiley-VCH, Weinheim, p 399
16. Wang X-M, Chen H-Y, Li S-Y, Wang J-D (1994) Anal Chim Acta 290:349–355
17. Carter MT, Rodriguez M, Bard AJ (1989) J Am Chem Soc 111:8901–8911
18. Kara P, Kerma K, Ozka D, Meric B, Erdem A, Ozkan Z, Ozsoz M (2002) Electrochem Commun 4:705–709
19. Yau HCM, Chan HL, Yang M (2003) Biosens Bioelectron 18:873–879
20. Marin D, Perez P, Teijeiro C, Palecek E (1998) Biophys Chemist 75:87–95
21. Piedade JAP, Fernandes IR, Oliveira-Brett AM (2002) Bioelectrochemistry 56:81–83
22. Cullis PM, McClymont JD, Symons MCR (1990) J Chem Soc Faraday Trans 86:591–592
23. Dohno C, Stemp EDA, Barton JK (2003) J Am Chem Soc 125:9586–9587
24. Hall DB, Barton JK (1997) J Am Chem Soc 119:5045–5046
25. Hall DB, Holmlin RE, Barton JK (1996) Nature 382:731–735
26. Vennerstrom JL, Makler MT (1995) Antimicrob Agents Chemother 39:2671–2677
27. Tuite E, Kelly JM (1995) Biopolymers 35:419–433
28. Shumakovich GP, Bachurin SO, Dubova LG, Zaitseva EA, Yaropolov AI (2001) Doklady Chem 377:114–117
29. Zhang G, Pang Y, Shuang S, Dong C, Choi MMF, Liu D (2005) J Photochem Photobiol A Chem 169:153–158
30. Cao Y, He X (1998) Spectrochim Acta 54A:883–892
31. Kim S, Jung S (1997) Bull Korean Chem Soc 18:1318–1320
32. Salomi BSB, Mitra CK, Gorton L (2005) Synth Met 155:426–429
33. Bard AJ, Faulkner LR (2001) Electrochemical methods. Wiley, New York, p 231
34. Pang D-W, Zhang M, Wang Z-L, Qi Y-P, Cheng J-K, Liu Z-Y (1996) J Electroanal Chem 403:183–188
35. Pang D-W, Abruna H (1998) Anal Chem 70:3162–3169
36. Meggers E, Michel-Beyerle ME, Giese B (1998) J Am Chem Soc 120:12950–12955
37. Delaney S, Barton JK (2003) J Org Chem 68:6475–6483
38. Kang J, Zhuo L, Lu X, Liu H, Zhang M, Wu H (2004) J Inorg Biochem 98:79–86
39. Kelley SO, Barton JK (1997) Bioconjug Chem 8:31–37